RELATION BETWEEN OFFSET AND VELOCITY DETERMINATION: APPLICATION ON A SYNTHETIC SEISMIC DATA SET FROM NORTHERN GHAWAR FIELD, SAUDI ARABIA

BY

Khalid Ahmed Abdulrahman

A Thesis Presented to the
DEANSHIP OF GRADUATE STUDIES

KING FAHD UNIVERSITY OF PETROLEUM & MINERALS

DHAHRAN, SAUDI ARABIA

In Partial Fulfillment of the
Requirements for the Degree of

MASTER OF SCIENCE

In

GEOPHYSICS

MAY, 2017

KING FAHD UNIVERSITY OF PETROLEUM & MINERALS

DHAHRAN- 31261, SAUDI ARABIA

DEANSHIP OF GRADUATE STUDIES

This thesis, written by **Khalid Ahmed Abdulrahman** under the direction of his thesis advisor and approved by his thesis committee, has been presented and accepted by the Dean of Graduate Studies, in partial fulfillment of the requirements for the degree of **MASTER OF SCIENCE IN GEOPHYSICS.**

Dr. Abdullatif Al-Shuhail
(Advisor)

Dr. Abdulaziz Al-Shaibani
Department Chairman

Dr. SanLinn Ismail Kaka
(Member)

Dr. Salam A. Zummo
Dean of Graduate Studies

Dr. Khalid Al-Ramadan
(Member)

4/2/2018
Date

Dedication

To My Father and Mother

To My Family

For Their Support and Love

ACKNOWLEDGMENTS

"In the name of Allah, The Most Gracious and The Most Merciful"

I would like to thank King Fahd University of Petroleum and Minerals (KFUPM) for giving me the opportunity to continue my higher studies.

My deepest appreciation and gratitude goes to my thesis advisor Dr. Abdullatif Al-Shuhail for his support, guidance, motivation and patience during my research. I also would like to express my deep gratitude to Dr. Abdulaziz Al Shaibani - the chairman of the Geosciences Department, and to Dr. SanLinn Ismail Kaka and Dr. Khalid Al-Ramadan for their support as my thesis committee members.

Special thanks go to Eng. Syed Abdul Salam for generating the synthetic seismic data, and to Mr. Ayman Al-Lehyani for his help while processing the data.

Finally, I would like to thank all the faculty and staff of the Geosciences Department, and the students with whom I interacted during my studies at KFUPM.

TABLE OF CONTENTS

LIST OF TABLES

LIST OF FIGURES

ABSTRACT

Full Name : Khalid Ahmed Abdulrahman

Thesis Title : RELATION BETWEEN OFFSET AND VELOCITY DETERMINATION: APPLICATION ON A SYNTHETIC SEISMIC DATA SET FROM NORTHERN GHAWAR FIELD, SAUDI ARABIA

Major Field : MASTER OF SCIENCE IN GEOPHYSICS

Date of Degree : 2017

In seismic surveys, seismic data processors usually try to make the offset as small as possible compared to the depth of investigation to reduce the errors when trying to calculate and analyze velocities. The short-offset assumption assumes that the offset is less than the depth (X<H).

In this research, I investigated the effect of offset on velocity analysis in a specific area of Ghawar Field. A viscoelastic depth model was used to generate viscoelastic synthetic seismic data using finite difference method. I processed the data using SU (Seismic Unix). After that, I estimated the interval velocity of a key layer (Biyadh) and compared it to the model value and quantified the errors in velocity estimation when offset is restricted versus when it is unrestricted.

My results showed - unlike what is expected by theory – that there is no need to honor the short-offset assumption when working on this particular area of Ghawar Field, as the difference in percentage between the average error in velocity estimation when offset is unrestricted versus when it is restricted is just 2.893%.

ملخص الرسالة

الاسم الكامل: خالد أحمد محمد عبدالرحمن

عنوان الرسالة: العلاقة بين الإزاحة و تقدير السرعات: تطبيق على بيانات سيزمية اصطناعية من شمال حقل الغوار بالمملكة العربية السعودية

التخصص: ماجستير علوم جيوفيزياء

تاريخ الدرجة العلمية: 2017

في المسوحات السيزمية (الزلزالية)، عادة ما يريد معالج البيانات السيزمية أن تكون الإزاحة (المسافة بين مصدر الموجات السيزمية و آخر المستقبلات) صغيرة قدر الإمكان مقارنة مع العمق المراد استكشافه. ويكون ذلك من أجل الحد من الأخطاء عند محاولة حساب وتحليل سرعات الموجات في الطبقات الأرضية. عادة ما يفترض أن الإزاحة أقل من العمق ($X < H$).

في هذا البحث، قمت بدراسة تأثير الإزاحة على تحليل السرعات في منطقة معينة من حقل الغوار. كان لدي نموذج السرعات الحقيقية، والذي تم استخدامه لتوليد البيانات السيزمية الاصطناعية ومن ثم معالجتها. و قد قمت بتقدير السرعة في إحدى الطبقات الرئيسية (بياض) ومقارنتها مع القيم في النموذج الأصلي لتحديد و مقارنة الأخطاء في تقدير السرعات عندما تكون الإزاحة مقيدة و غير مقيدة.

النتائج أظهرت – بخلاف ما هو متوقع نظريا – أنه ليس بالضرورة أن تكون الإزاحة أقل من العمق في المنطقة التي تمت دراستها من حقل الغوار. حيث أن الفرق في النسبة المئوية بين الأخطاء المحتسبة في حالة عدم تقييد الإزاحة و حالة تقييد الإزاحة هو 2.893 % فقط.

CHAPTER 1
INTRODUCTION

In seismic exploration, seismic velocities are the most important parameters that can be derived from the time-distance curves, which are referred to as T-X curves (where T is the two-way travel time and X is the offset of investigation). This is because they are used in many steps of seismic data processing such as: spherical divergence correction, normal moveout (NMO) correction and stacking, interval velocity determination, migration, time to depth conversion, etc.

There are many types of seismic velocities. The most important ones which are the focus of this research are the root-mean-square (V_{RMS}) and stacking (V_S) velocities.

1.1 What are RMS, Stacking, and Interval Velocities

V_{RMS} can be defined to the bottom of the N^{th} layer in a series of N plane horizontal homogeneous layers as the reciprocal of the square root of the coefficient of X^2 that I get when fitting an infinite polynomial to the true $T^2 - X^2$ curve.

To further illustrate the meaning of this definition, let us look at the following equations which give us the exact offset (X) and two-way traveltime (T_N) to the bottom of the N^{th} layer in a series of plane horizontal homogeneous layers (Sheriff & Geldart, 1995):

$$X = 2\sum_{i=1}^{N} \frac{pV_i H_i}{\sqrt{1-(pV_i)^2}} \quad , \qquad (1.1)$$

$$\text{and } T_N = 2\sum_{i=1}^{N} \frac{H_i}{V_i\sqrt{1-(pV_i)^2}} \qquad (1.2)$$

where:

V_i is the interval velocity of the i^{th} layer

H_i is thickness of the i^{th} layer

$p=dT_N/dX$ is the parameter of the ray received at X with $T = T_N$

However, Taylor series expansion about X=0 (Maclaurin series expansion) can be used to represent the exact T_N in terms of X which will give us the following curve:

$$T_N{}^2(X) \approx \sum_{k=0}^{\infty} C_k X^{2k} = C_0 + C_1 X^2 + C_2 X^4 + \cdots \qquad (1.3)$$

which will converge to the exact T – X curve under two conditions:

1- $C_K X^{2k}$ goes to 0 as k goes to infinity, which can be accomplished by not violating the short-offset assumption ($X_{max} < H_{\text{to the Nth Layer}}$)

2- Using an infinite number of terms (k goes to infinity)

I will get the following equations if infinite number of terms is used in equation (1.3):

$$T_N{}^2(X = 0) = C_0 = \left[\sum_{i=1}^{N} \frac{2H_i}{V_i}\right]^2 = \left[\sum_{i=1}^{N} \Delta t_i\right]^2 = T_N(0)^2 \qquad (1.4)$$

$$\text{and } C_1 = \left[\frac{\sum_{i=1}^{N} \Delta t_i}{\sum_{i=1}^{N} V_i{}^2 \Delta t_i}\right] = \frac{1}{(V_{RMS\,N})^2} \qquad (1.5)$$

where:

Δt_i is the two-way zero-offset interval traveltime across the i^{th} layer

$V_{RMS\,N}$ is the RMS velocity to the bottom of the N^{th} reflector

It can be seen from equation (1.5) that V_{RMS} can be calculated directly in terms of the properties of subsurface layers by:

$$V_{RMS\,N} = \left(\frac{\sum_{i=1}^{N} V_i{}^2 \Delta t_i}{\sum_{i=1}^{N} \Delta t_i}\right)^{1/2} \qquad (1.6)$$

Moreover, from equation (1.5) it can be seen that that V_{RMS} can also be defined as the reciprocal of the square root of the coefficient of X^2 that I get when fitting a polynomial to the true $T^2 - X^2$ curve in an infinite series expansion:

$$V_{RMS\,N} = \frac{1}{\sqrt{C_1}} \qquad (1.7)$$

If the I truncate the series after two terms, I will get the stacking velocity instead of V_{RMS}. Note that when truncating after two terms I get an equation of a hyperbola.

Thus, stacking velocity is defined as the velocity found by fitting a hyperbola to the true T-X curve. This fitting will give absolute error-free results in case the true ray path follows a straight line. However, this is not a realistic case if the ray passes through multiple layers. Ray path deviates further from a straight ray path as the offset of investigation increases. This is illustrated in Figure 1.1:

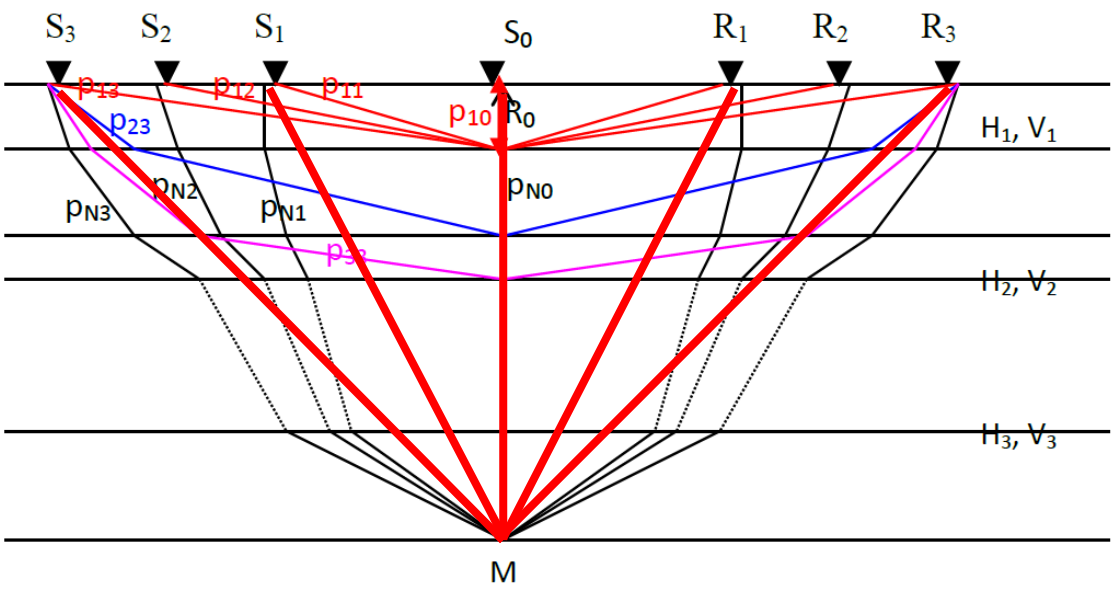

Figure 1.1: Ray path deviation from straight line (red lines) as offset increases (Al-Shuhail, 2017)

Figure 1.1 shows a configuration of different sources (S_0, S_1, S_2, S_3) and different receivers (R_0, R_1, R_2, R_3) in a typical seismic exploration project over multiple layers. Each layer has a different velocity (V) and thickness (H), so each ray has a different ray parameter (P_{ik} reflected from the i-th reflector and recorded by the k-th receiver).

RMS or stacking velocity can be used in a formula proposed by Dix (1955) to calculate interval velocities. I will use the stacking velocity in this study.

Dix Formula states that the interval velocity of the N^{th} layer can be calculated from the RMS or stacking velocities as follows:

$$V_{Dix} = \sqrt{\frac{V_N^{\,2}\, T_N \;-\; V_{N-1}^{\,2}\, T_{N-1}}{T_N \;-\; T_{N-1}}} \qquad (1.8)$$

where V_{N-1} and V_N are the velocities (RMS or stacking) to the top and bottom of the N^{th} layer, and T_{N-1} and T_N are the total traveltimes to the top and bottom of the N^{th} layer.

The aim of this research is to quantify the error in interval velocity calculation in Northern Ghawar Field as the violation of the short-offset assumption increases.

1.2 Statement of Problem

It is very common in practice to record beyond the short-offset assumption in modern seismic acquisition. Some processors tried to use the data obtained from far offsets to calculate velocities, but it is not quite straightforward or accurate as using the data from short offsets.

Most of the time, the whole offset range of the data is used for velocity with no regard to the short-offset assumption. The objective of this research is to estimate the error in interval velocities with and without honoring the short-offset assumption in Northern Ghawar Field.

1.3 Literature Review

For accurate structural interpretation and lithological information, Dix (1955) developed a formula in order to determine seismic interval velocities accurately prior to drilling. His formula calculates interval velocity from RMS velocities as shown in equation (1.8).

For isotropic, homogeneous, and layered media, the hyperbolic approximation of RMS velocity was extended by deriving a higher-order series by Taner and Koehler (1969) as shown in equation (1.3).

When using two terms in the series, it is called stacking velocity. It is possible that using more terms may enhance velocity estimation. However, instead of having an infinite number of terms, as proposed in the original series, it is better for practical applications to truncate the expansion after the third term. This was shown by many authors such as Shah and Levin (1973) who found out that the errors made by truncation after the third term were less than 2 percent. Al-Chalabi (1974) also showed the same when analyzing stacking, RMS, average, and interval velocities over a horizontally layered ground. He also showed that long-offset spreads could lead to large errors in velocity determination. Hake et al. (1984) also used three terms when trying to study the relationship between the true velocities of a transversely isotropic layer and velocities calculated from $T^2 - X^2$ curves.

Unfortunately, even with more terms, the Taner and Koehler (1969) series converges only under short offsets since the true ray path deviates further from a straight ray path as the offset of investigation increases. According to Al-Chalabi (1973), adding more terms in the series for very large offsets can increase the errors in velocity estimation instead of decreasing them as the series rapidly converges but strong oscillations can be observed.

Causse et al. (2000) studied large-offset approximations to seismic reflection traveltimes. They presented a new approximation which gives much better results at large offsets. Their approximation was in a form of a series containing powers of the offset from 1 to $-\infty$. However, they show that their new approximation is inaccurate at short offsets and gives great errors.

In this study, the model velocities and densities values used to estimate errors in interval velocity calculation with and without honoring the short-offset assumption in Northern Ghawar Field were taken from a realistic subsurface geological model. This model was built in order to select suitable formations for CO2 injection in eastern Saudi Arabia (Al-Shuhail et al., 2014). The model values were used to generate synthetic seismic data using 2D viscoelastic finite difference wave field modeling method (Thorbecke, 2017).

CHAPTER 2

MODEL AND DATA GENERATION

2.1 Study Area

Ghawar Field is the largest onshore oil field in the world. An area in northern Ghawar Field between Ain Dar and Shudgam was studied in this work (Figure 2.1).

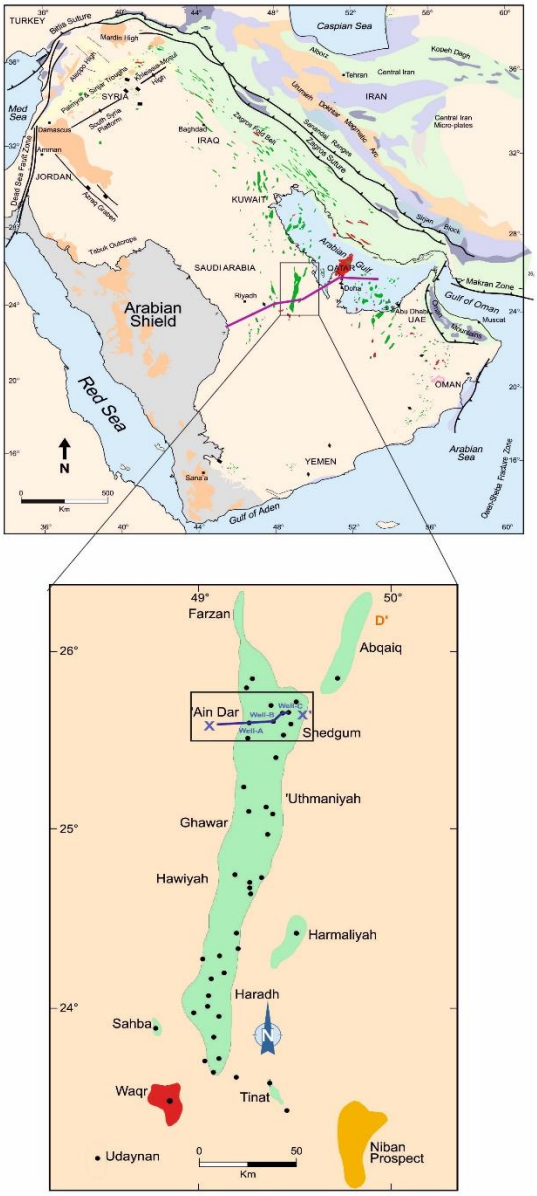

Figure 2.1: Location of the study area (Al-Shuhail et al., 2014)

Figure 2.2 shows the stratigraphy under the study area. In addition, it shows Vp (which is the velocity of the P-wave where the particle motion in a medium affected by the wave is parallel to the wave propagation direction), Vs (which is the velocity of the S-wave where the particle motion in a medium affected by the wave is perpendicular to the wave propagation direction), and ρ (which is density) values for most formations in the model.

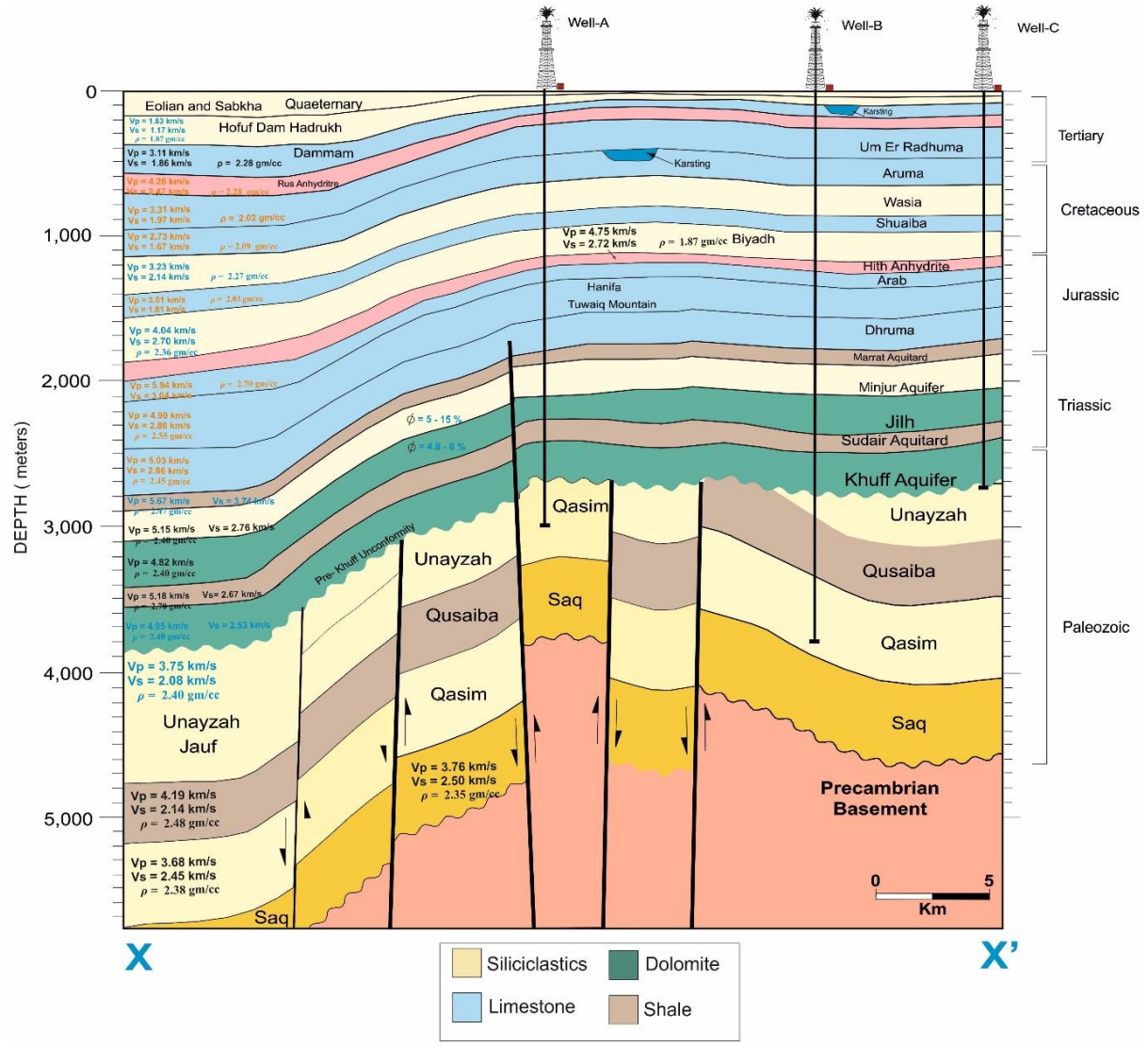

Figure 2.2: Stratigraphy, densities, and velocities in the study area (Al-Shuhail et al., 2014)

2.2 Digitization

Digitization is the first step in generating seismic data. I digitized the data using a software called Digitizeit (http://www.digitizeit.de/).

To digitize, I uploaded Figure 2.2 and defined the axes and their minimum and maximum values. The software followed lines and curves on the image automatically or manually and assigned X and Y values to each point on the lines or curves. Those X and Y values were then extracted to an Excel Sheet to redraw the image and work on it.

Figure 2.3 shows the output model after digitization:

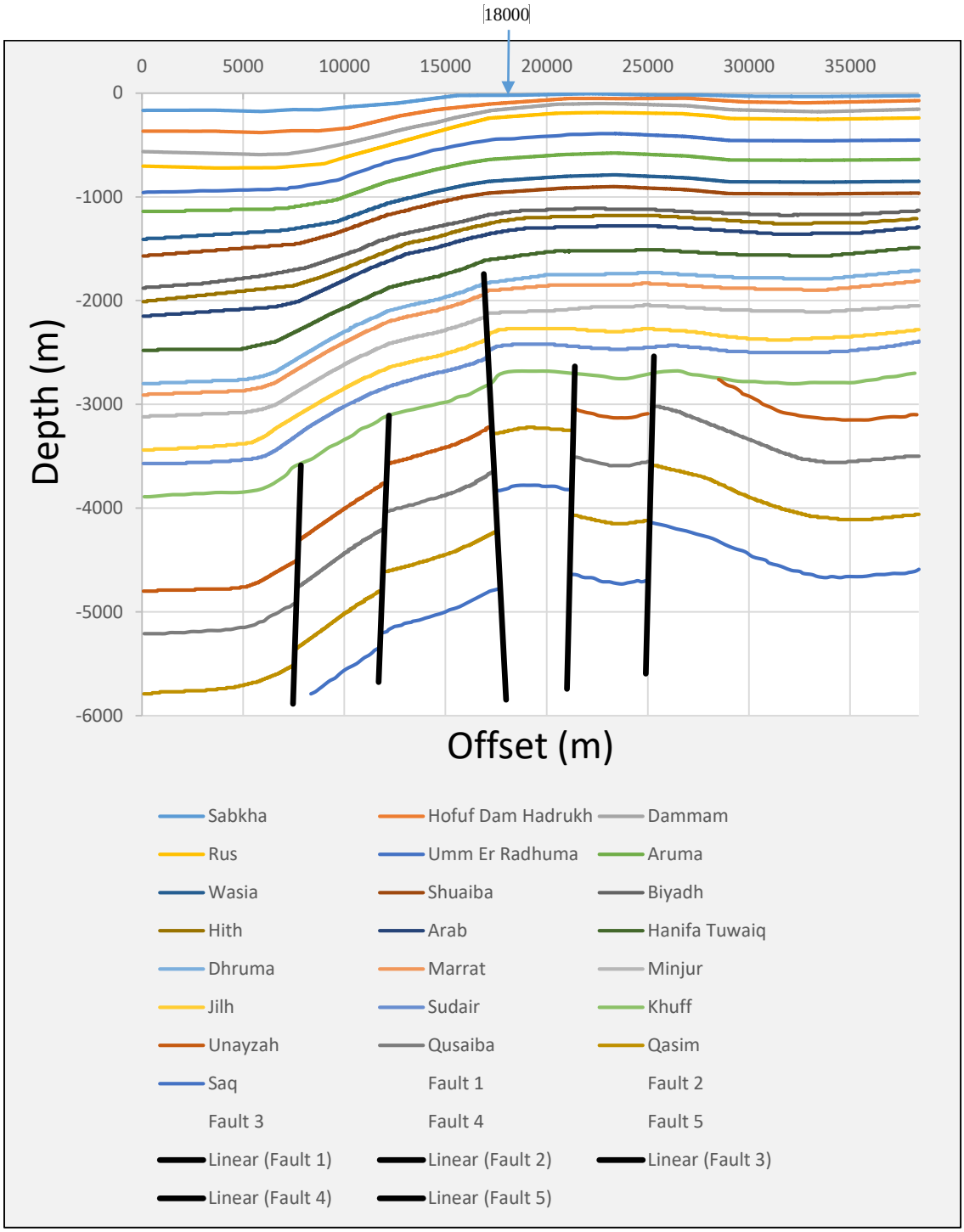

Figure 2.3: Digitized model

2.3 Model Velocities, Depths, Thicknesses, and Two-Way Travel Times

In this study, I focused on the layer Biyadh to compare my calculated velocities with the correct ones from the model. Biyadh was selected because it is a relatively thick layer (197 meters) and have a high velocity (4045 m/s) compared to Shuaiba (which is the layer above Biyadh with a velocity 3010 m/s). Those two factors make it more suitable to calculate the right velocity for the layer. Table 2.1 shows model (true) velocities and densities of each layer from the model.

#	Formation	Average Vp (m/s)	Average Vs (m/s)	Average ρ(gm/cc)
0	Quaternary	850	501.9	1.5
1	Hofuf Dam Hadrukh	1835.0	1179.8	1.9
3	Dammam	3110.0	1869.7	2.3
2	Rus	4267.0	2471.4	2.3
4	Umm Er Radhuma	3318.0	1977.9	2.0
5	Aruma	2730.0	1672.1	2.1
6	Wasia	3233.0	2141.9	2.3
7	Shuaiba	3010.0	1817.7	2.0
8	Biyadh	4045.0	2700.8	2.4
9	Hith Anhydrite	4483.0	2327.5	3.0
10	Arab	5398.5	2748.0	2.7
11	Hanifa	5697.5	2903.0	2.6
12	Dhruma	5033.0	2869.7	2.5
13	Marrat	3344.0	1465.0	2.3
14	Minjur	5154.0	3464.0	2.5
15	Jilh	4823.0	2760.5	2.4
16	Sudair	5182.0	2674.0	2.4
17	Khuff	4953.0	2530.0	2.7
18	Unayzah	3752.0	2085.0	2.4
19	Qusaiba	3898.0	2143.0	2.5
20	Qasim	3685.0	2453.0	2.4
21	Saq	3765.0	2508.1	2.4
22	Basement	6380.0	3580.0	2.8

Table 2.1: True velocities and densities

From the digitized model, I estimated the depth (Z) and thickness (H) of each layer at any point along the line. Table 2.2 shows depth and thickness of each layer at 18000 m.

#	Formation	Z (m) (at X=18000 m)	H (m) (at X=18000 m)
0	Quaternary	21	21
1	Hofuf Dam Hadrukh	94	73
3	Dammam	153	59
2	Rus	228	75
4	Umm Er Radhuma	442	214
5	Aruma	629	187
6	Wasia	840	211
7	Shuaiba	953	113
8	Biyadh	1150	197
9	Hith Anhydrite	1230	80
10	Arab	1330	100
11	Hanifa	1580	250
12	Dhruma	1800	220
13	Marrat	1890	90
14	Minjur	2110	220
15	Jilh	2280	170
16	Sudair	2430	150
17	Khuff	2690	260

Table 2.2: True depth and thickness of each layer at X=18000 m.

Reasons for doing the calculations at X=18000 m is discussed in Chapter 4.

I used H and average Vp from the previous two tables to calculate the two-way travel times (ΔTi) of each layer which equals 2H/Vp. Then, I calculated the two-way travel times form the surface to the bottom of each layer (∑ ΔTi). The results are shown in Table 2.3.

#	Formation	ΔTi (s) (at X=18000 m)	∑ ΔTi (s) (at X=18000 m)
0	Quaternary	0.050	0.050
1	Hofuf Dam Hadrukh	0.080	0.129
3	Dammam	0.038	0.167
2	Rus	0.035	0.202
4	Umm Er Radhuma	0.129	0.331
5	Aruma	0.137	0.468
6	Wasia	0.131	0.599
7	Shuaiba	0.075	0.674
8	Biyadh	0.097	0.771
9	Hith Anhydrite	0.036	0.807
10	Arab	0.037	0.844
11	Hanifa	0.088	0.932
12	Dhruma	0.087	1.019
13	Marrat	0.054	1.073
14	Minjur	0.085	1.159
15	Jilh	0.070	1.229
16	Sudair	0.058	1.287
17	Khuff	0.105	1.392

Table 2.3: True two-way travel times

It can be seen from Table 2.3 that the two-way travel times from the surface to the top and bottom of Biyadh are 0.674 s and 0.771 s, respectively.

2.4 Data Generation

After digitization, seismic data sets of SU format were generated utilizing the P-wave velocity (Vp), S-wave velocity (Vs), P-wave quality factor (Qp), S-wave quality factor (Qs), and density (ρ) values from my model. The quality factors (Qp, and Qs) are used to account for the influence of attenuation in dissipative media.

The software used to do this is an open source program called: " 2D acoustic/visco-elastic finite difference wavefield modeling" or simply "fdelmodc" by Jan Thorbecke (https://janth.home.xs4all.nl/Software/Software.html).

The finite-difference methods are used in order to solve differential equations. This is done by approximating the differential equations with difference equations where finite differences approximate the derivatives.

In order to model and generate the data, the program "fdelmodc" uses finite difference in order to compute a solution of the 2D wave equation. The wave equation is defined through the first-order linearized systems of Hooke's and Newton's law. For a visco-elastic medium – just like my case – eight equations are used (Thorbecke, 2017).

In general, the program can be used to model waves in acoustic, visco-acoustic, elastic, and visco-elastic mediums. Where:

- In acoustic: only Vp, and ρ are taken into account.
- In visco-acoustic: Vp, Qp, and ρ are taken into account
- In elastic: Vs, Vs, and ρ are taken into account.
- In visco-elastic: Vp, Vs, Qp, Qs, and ρ are taken into account.

Figures 2.4 through 2.8 show the Vp, Vs, Qp, Qs, and ρ models in the study area:

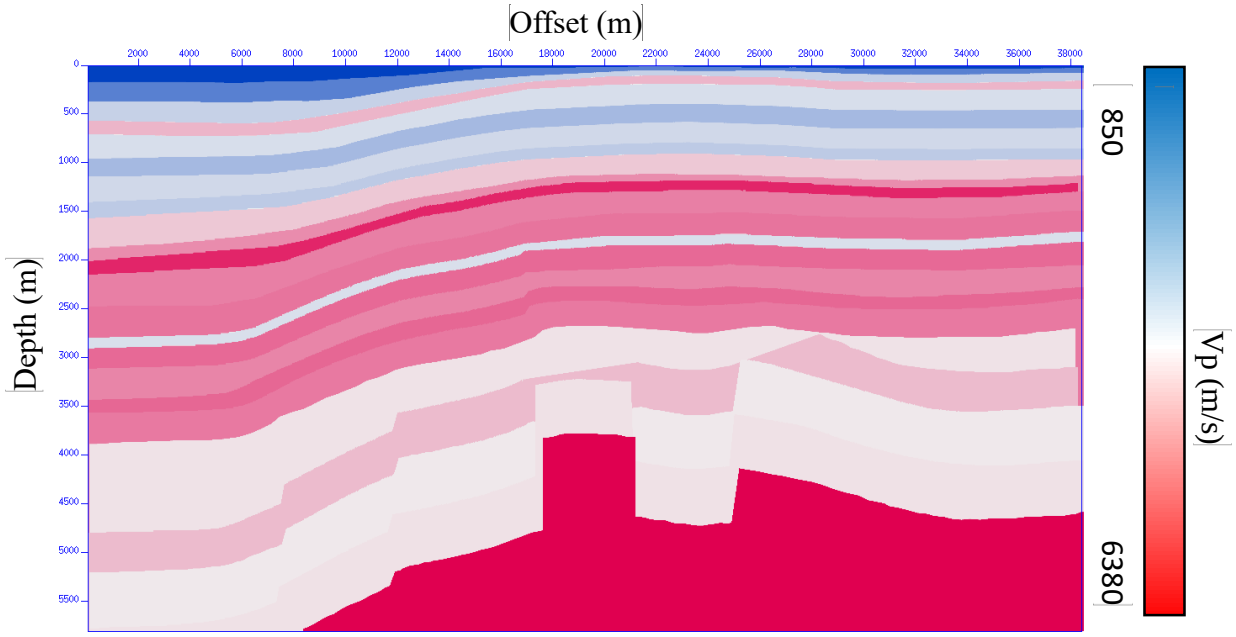

Figure 2.4: Vp model

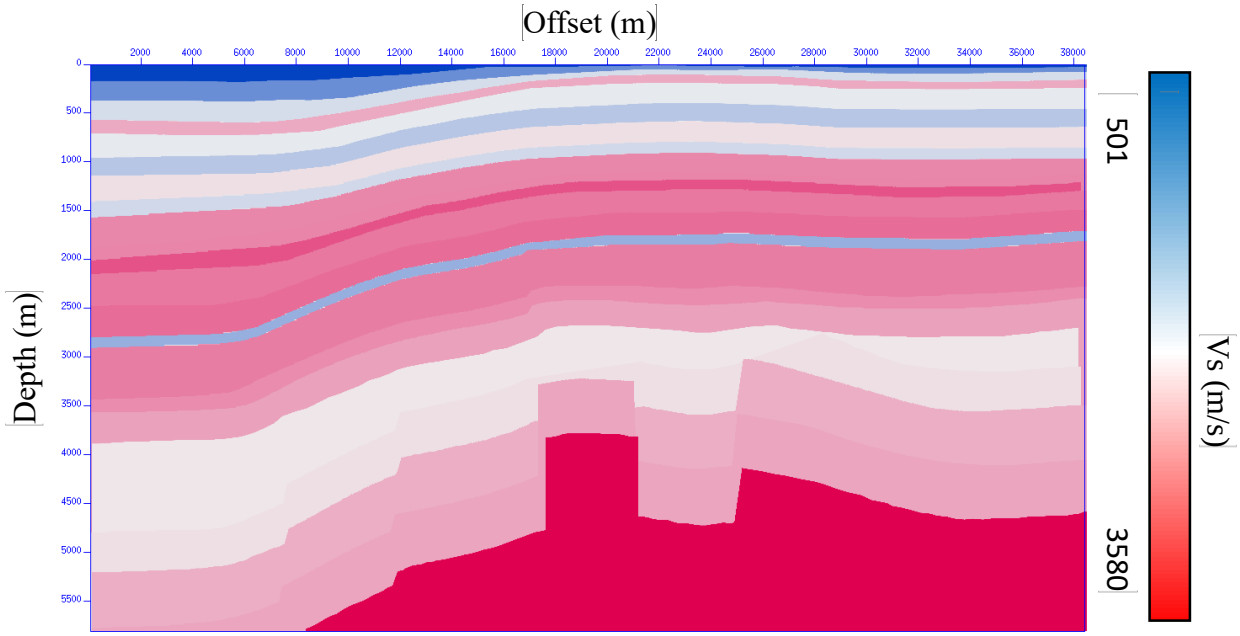

Figure 2.5: Vs model

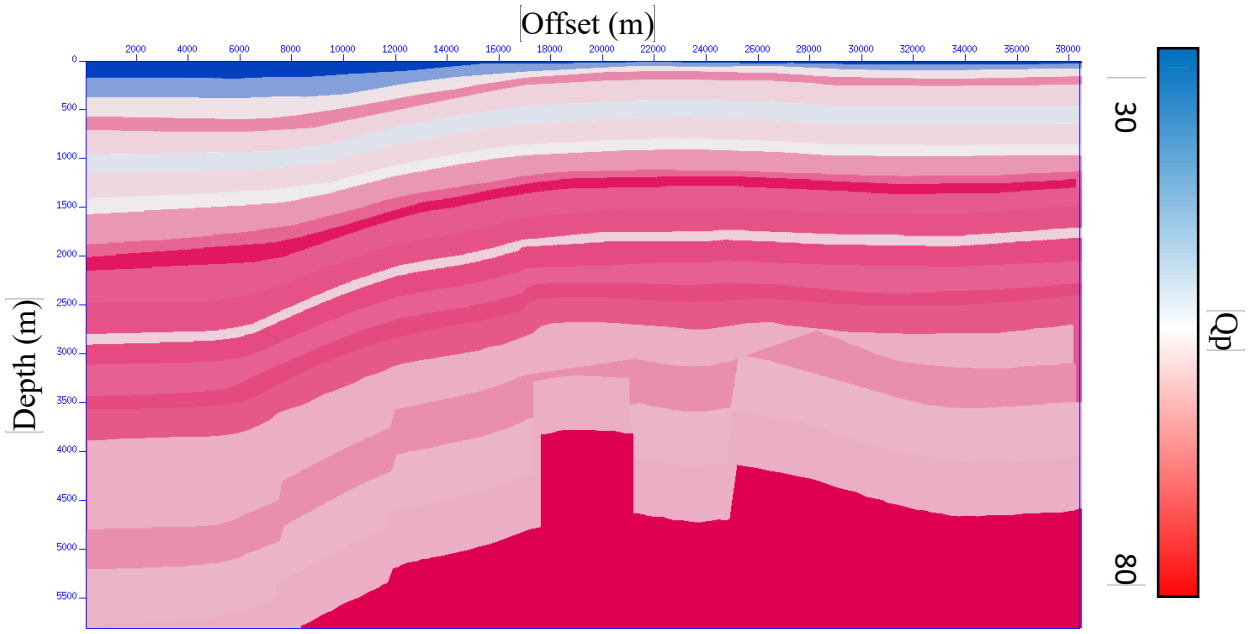

Figure 2.6: Qp model

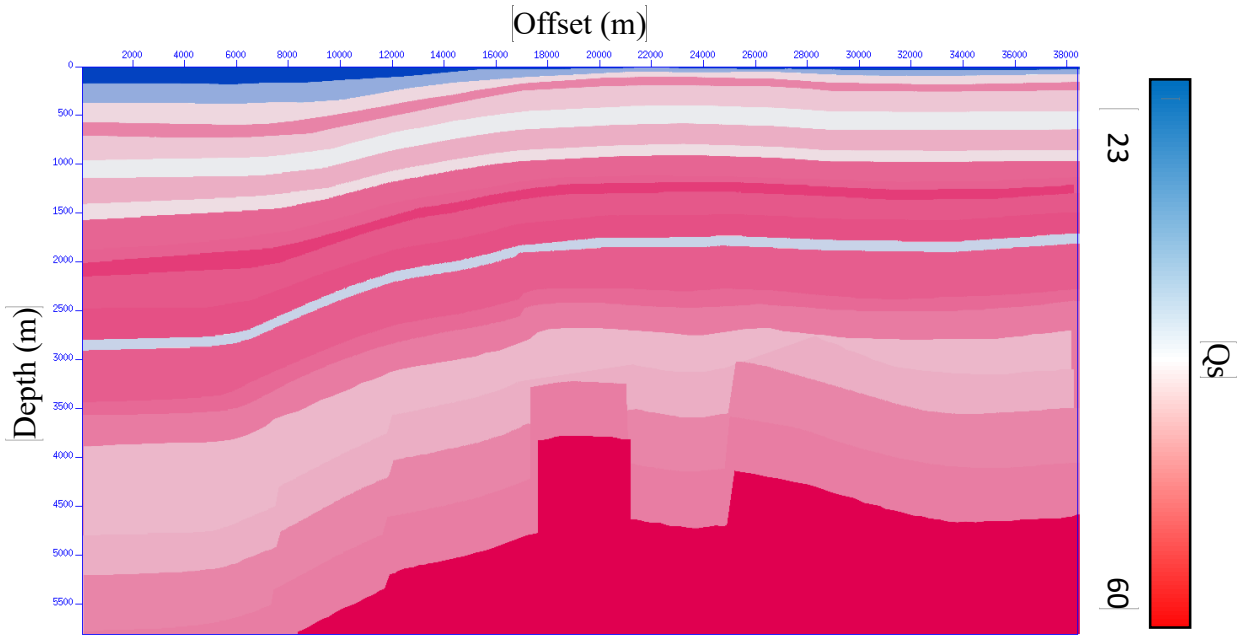

Figure 2.7: Qs model

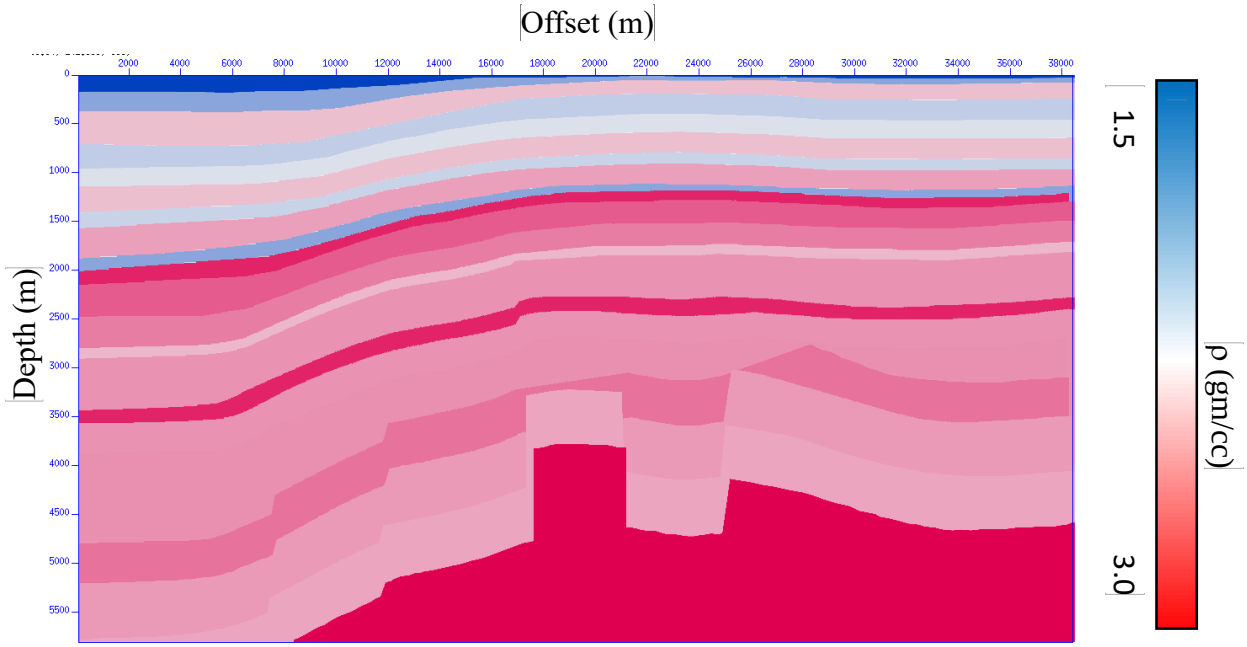

Figure 2.8: Density model

2.5 Synthetic Seismic Data Parameters

Table 2.4 lists important parameters about the synthetic seismic data and geometry used to generate it.

Wave Equation Type	2D viscoelastic
Record Length	6 seconds
Receiver Spacing	25 m
Shot Spacing	50 m
Source Wavelet Type	Zero Phase Ricker Wavelet
Dominant Frequency	25 Hz
Additive Noise	Gaussian noise with standard deviation of 10% and 0 Mean
Number of Traces	1178880
Maximum CDP Fold	768
Offset	- 38300 to 38350 m
Source Location	50 to 38350 m
Receiver location	50 to 38400 m
Number of Samples	1501
Sample interval	4 ms
Size	7.188 GB

Table 2.4: Synthetic data specifications

CHAPTER 3
DATA PROCESSING

Raw shot gathers have low signal-to-noise ratio and low resolution (Figure 3.1 shows the original data set before processing). They cannot be used directly to represent the subsurface. Therefore, seismic data must be processed to produce the best possible subsurface image which can be used by seismic interpreters to extract useful geologic information.

In general, seismic data processing is required to achieve the following goals:

- Enhancing the seismic resolution
- Increasing the signal-to-noise ratio
- Produce and image that represent the subsurface correctly

The processing steps I used in this research are the following:

- Gain application
- Filtering
- Deconvolution
- CDP sorting
- Velocity analysis

Velocity analysis is an important part of seismic processing, and in this study I processed the data – using Seismic Unix – to the point that I can do the velocity analysis correctly in order to determine the seismic velocities of each layer of my model.

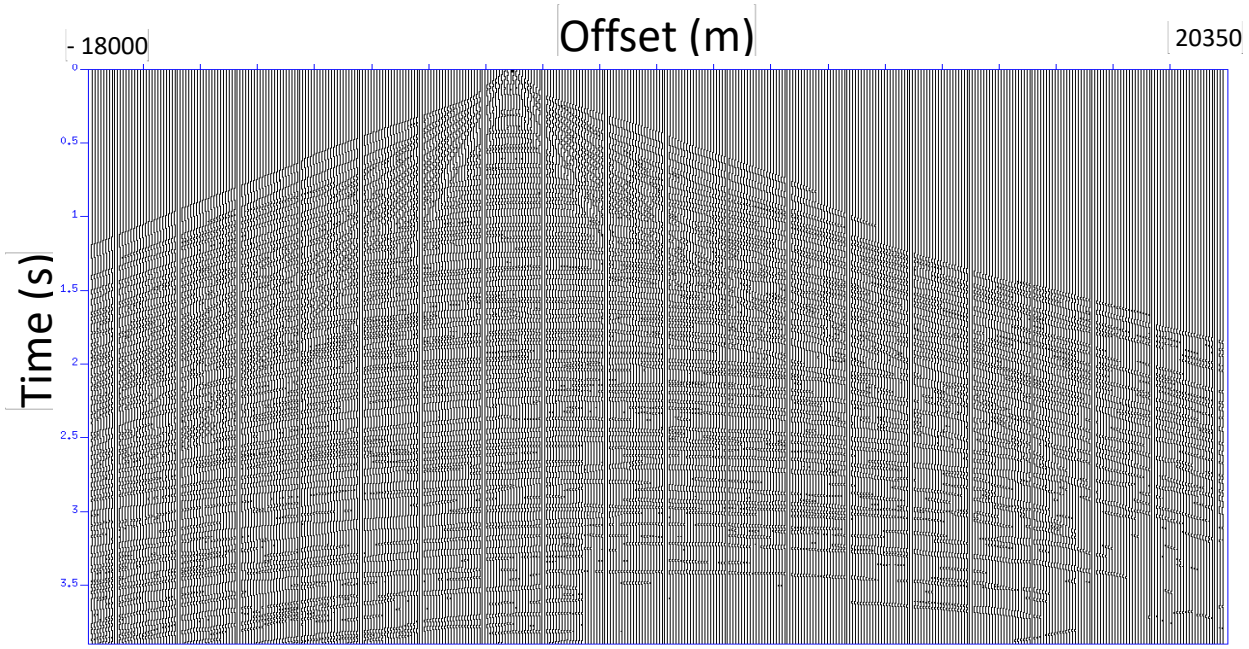

Figure 3.1: The original data set before processing (raw shot gather)

Following is an explanation of the steps taken (till velocity analysis) in order to process the data:

3.1 Gain application: The objective here was to account for amplitude loss due to spherical divergence and absorption.

This was done using T^2 gain method.

Important parameters used are summarized the table below:

Parameter	Value	Justification
AGC gate length	0.5 s	Most practical Value which gives well-balanced amplitudes at all times
Power of T	2	Best value to account for both spherical divergence and absorption (Yilmaz, 2001)

Figure 3.2 shows the data after gain application:

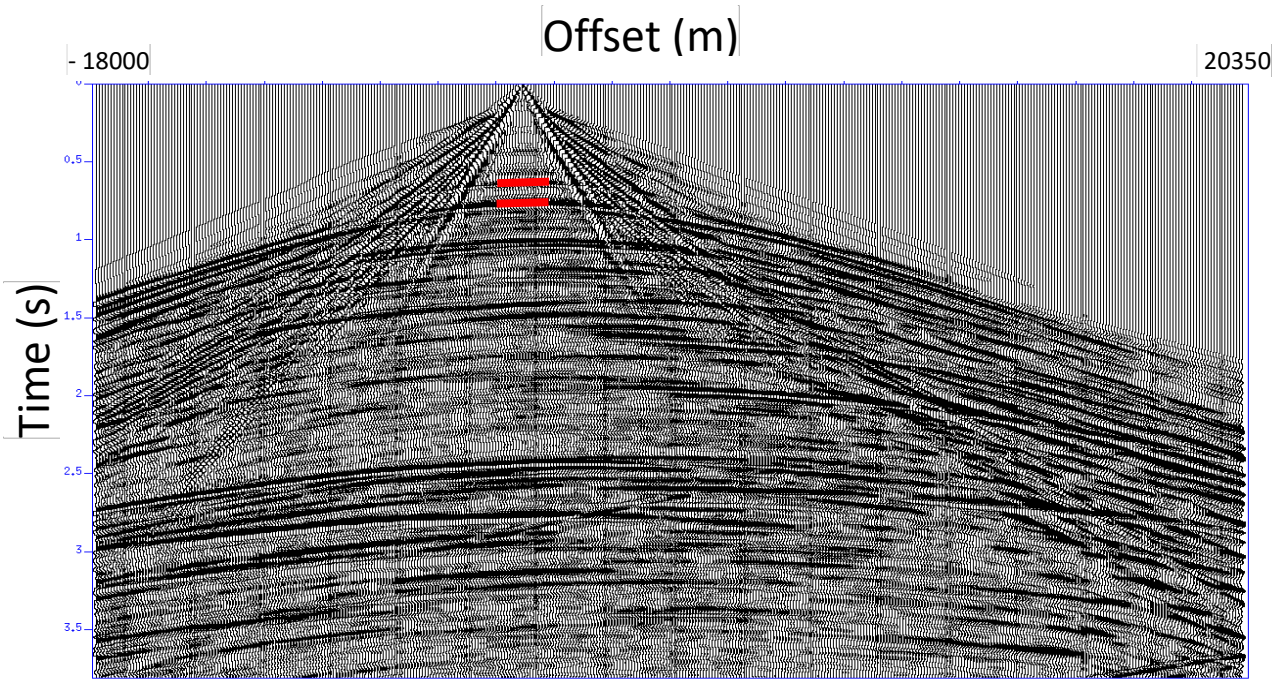

Figure 3.2: The data after gain using T^2 method (top and bottom of Biyadh are shown in red)

3.2 Fourier Transform: The objective is to display the amplitude spectrum of the data to be able to select the correct parameters when doing the frequency filtering in the next step.

Figure 3.3 shows the output after Fourier Transform:

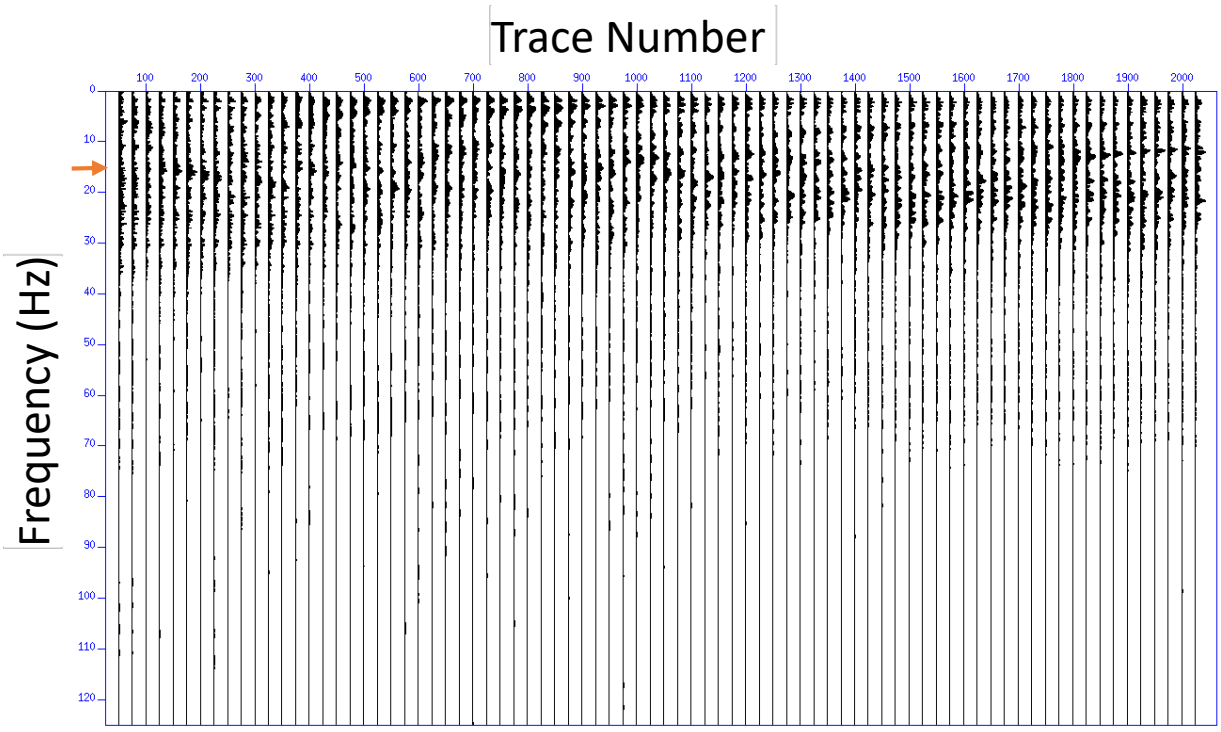

Figure 3.3: Amplitude spectra of traces displayed after Fourier Transform. The arrow indicates the end of the ground roll window

3.3 Filtering: The objective is to filter out the ground roll noise from the data using band-pass filer.

Important parameters used are summarized the table below:

Parameter	Value	Justification
Frequency Range Parameters	10,15,45,55 (Hz)	In my case, those are the best values to give an output which contains only frequencies that lie within my desired frequency range after removing ground roll. This was found from the amplitude spectra

Figure 3.4 shows the data after filtering:

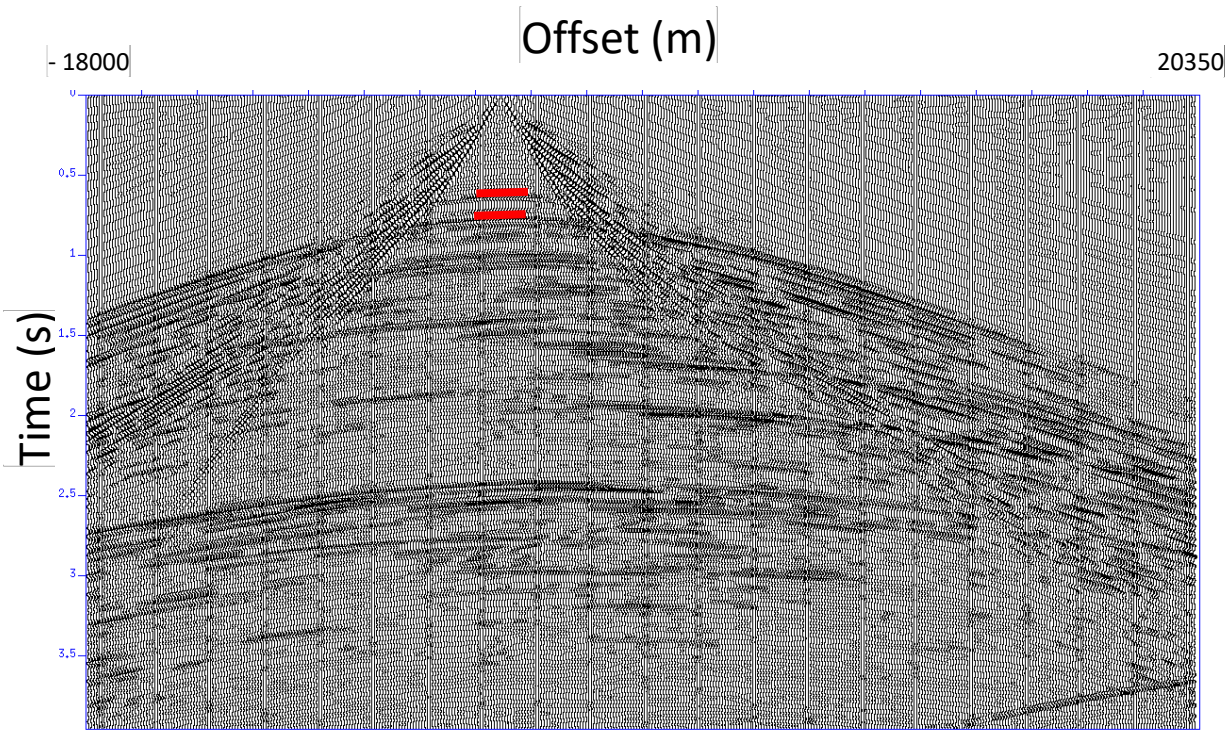

Figure 3.4: The data after filtering (top and bottom of Biyadh are shown in red)

3.4 Deconvolution: It is done to spike the data and increase the vertical resolution and to remove multiples. I also had to autocorrelate the data first to be able to correctly select the type and parameters of the deconvolution. Important parameters used are summarized the table below:

Parameter	Value	Justification
prediction lag parameter (α)	0.004 s	For spiking deconvolution
operator length parameter (n)	0.2 s	Should be as large as possible but not less than the length of the first transient zone of the trace autocorrelation, which is more than 0.2 s in this case
percent prewhitening parameter (ε)	0.001	In practice, 0.1% prewhitening is standard in processing
Minimum of the autocorrelation window	0 s	I need to set the autocorrelation window from the start of the record
Maximum of the autocorrelation window	6 s	I need to set the autocorrelation window till the end of the record

Figures 3.5 and 3.6 show the data after autocorrelation and after deconvolution.

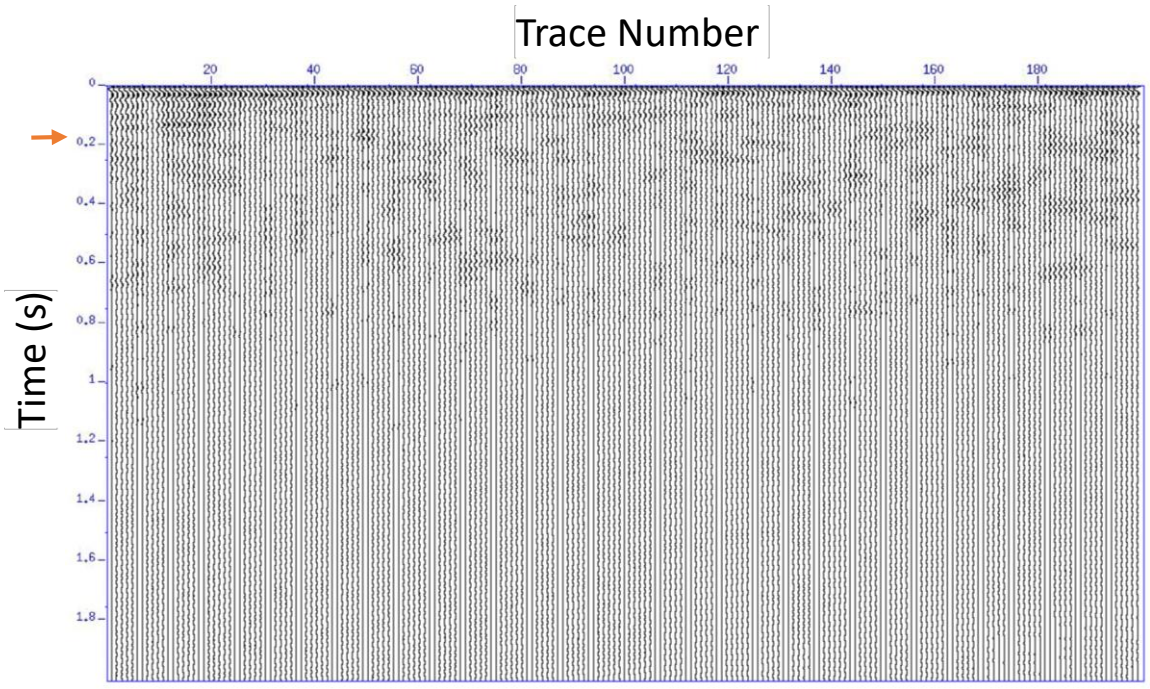

Figure 3.5: The data after autocorrelation. The arrow indicates the length of the first transient zone

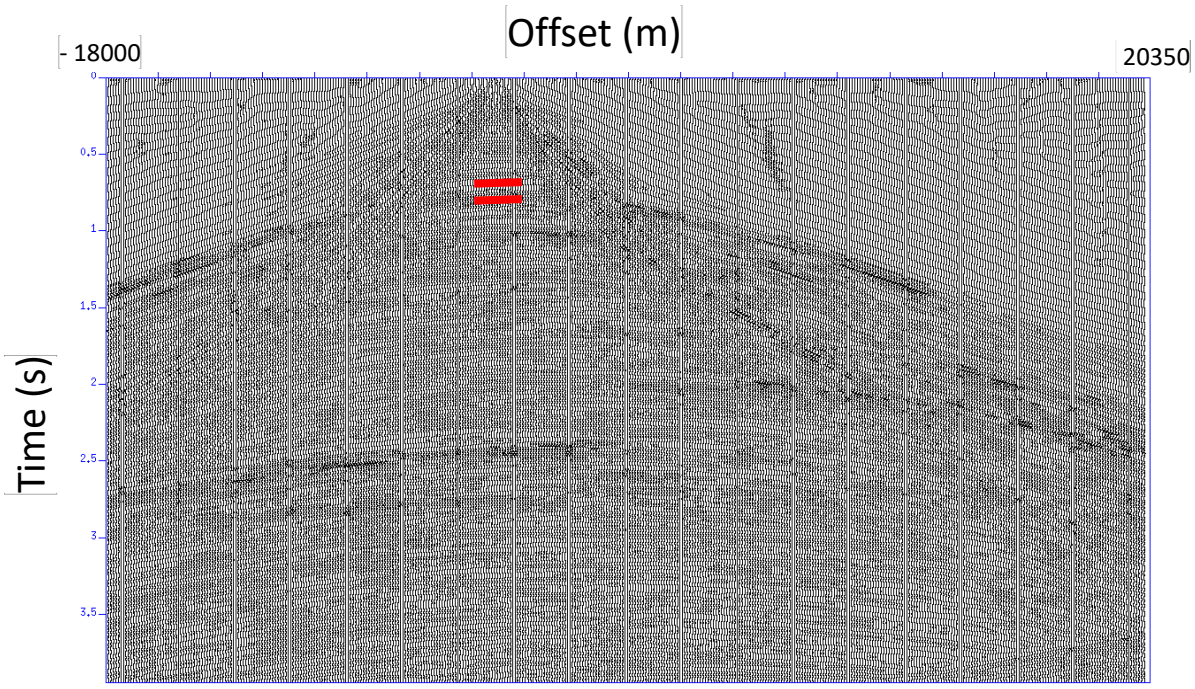

Figure 3.6: The data after deconvolution (top and bottom of Biyadh are shown in red)

3.5 Gain: The objective is to balance the amplitudes after deconvolution. Important parameters used are summarized the table below:

Parameter	Value	Justification
Clipping Quantile	0.95	My profile has less than 5% noisy points. Therefore, I clipped at the 95^{th} percentile. Traces are balanced by that percentile and scaled.

Figure 3.7 show the data amplitude balancing:

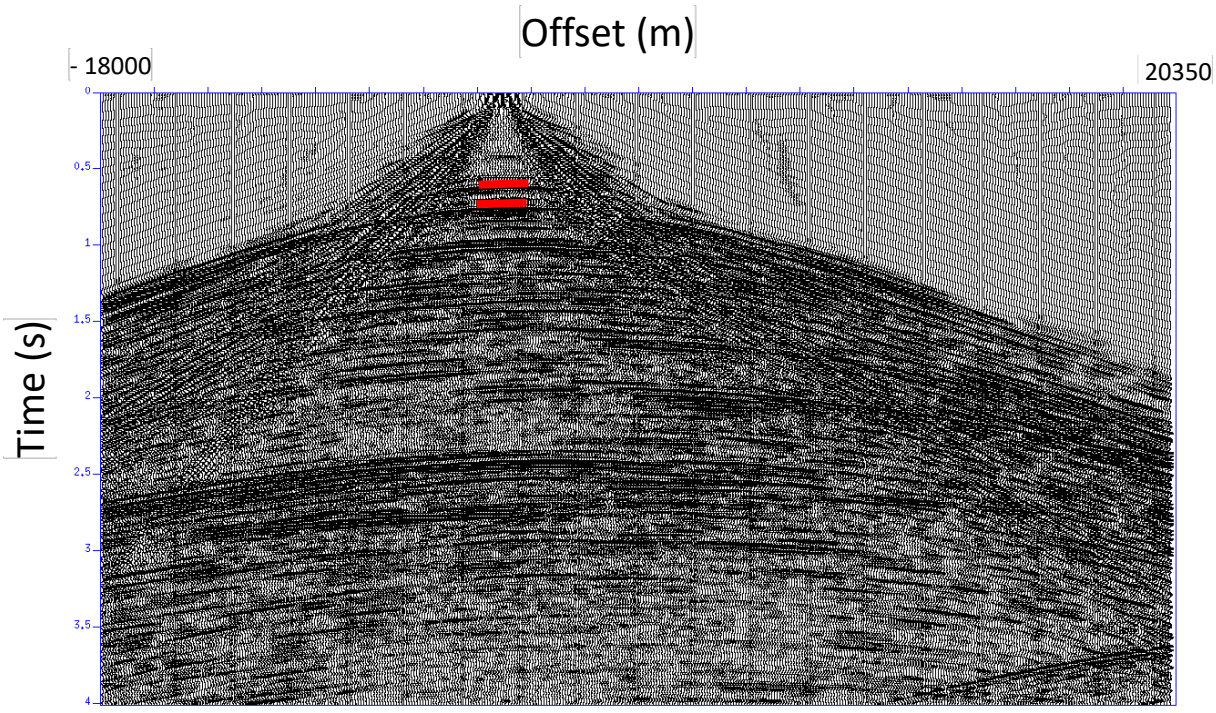

Figure 3.7: After deconvolution and amplitude balancing (top and bottom of Biyadh are shown in red)

3.6 CDP Sorting: Sorting the data from shot to common depth points (CDPs) gathers must be done before doing the velocity analysis in the next step. That is because picked velocity function only represents the subsurface at a specific location.

Figure 3.8 shows the data after CDP sorting:

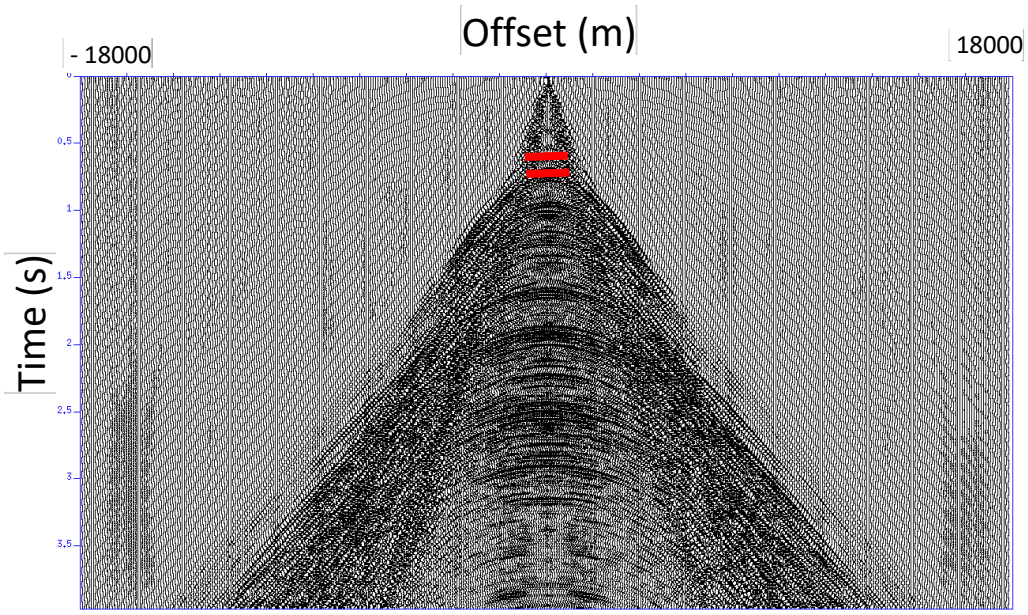

Figure 3.8: After CDP sorting (CDP at 18000 m)

3.7 Velocity Analysis:

Velocity analysis is done to determine the stacking velocity (which is assumed to be equal to the NMO and RMS velocities at short offsets). As mentioned in Chapter 2, the focus in this experiment was on the Biyadh formation.

There are many ways for velocity determination, and the one I used is the velocity spectrum in which a CDP is selected to end up with velocity values for each layer at that CDP. A CDP with high signal to noise ratio must be selected. Therefore, I selected CDP number 180000 - that is almost in the middle of the data at offset 18000 m - which has a large fold of 720 traces. Furthermore, the layers at 18000 m are not dipping, which makes it easier to study the effect of offset on velocity determination.

In Seismic Unix, I used the Velan script that uses suvelan command to do the velocity analysis. The script gives us a velocity spectrum of a specific CDP where the correct velocity that should be picked is one associated with maximum semblance – which is a measure of coherency - occurring at a specific time.

However, because of the subjectivity of the picking, I repeated this experiment 20 times to make sure that my results are statistically significant. Note that important parameters to set when using this method to cover all possible velocities are: first velocity, velocity increment, and number of velocities. In my experiment they were set to 500 m/s, 50 m/s, and 101 velocities, respectively.

I produced two sets of data. One where the full offset of the shots is taken into consideration at CDP180000, and one with short offset. To honor the short offset assumption when analyzing Biyadh formation (at a depth of 950 m) I only needed to use 76 traces or less centered around the source because (950m/25m)*2=76 where 25 m is the receiver spacing.

Moreover, I cut and use only the first two seconds of my data since I do not need the rest which is for much deeper layers.

Figures 3.9 and 3.10 show CDP 180000 without and with offset restriction:

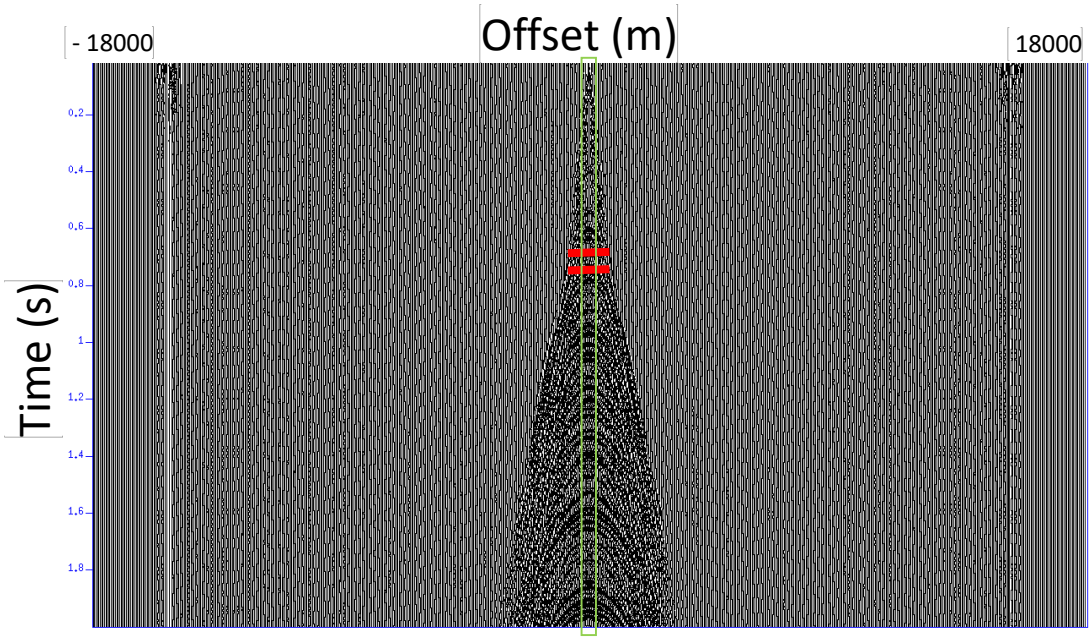

Figure 3.9: The first 2 seconds showing CDP 180000 when the entire offset is used. Top and bottom of Biyadh are shown in red. Data taken into consideration for the short offset case - which is enlarged in Figure 3.10 - is shown in the green rectangle

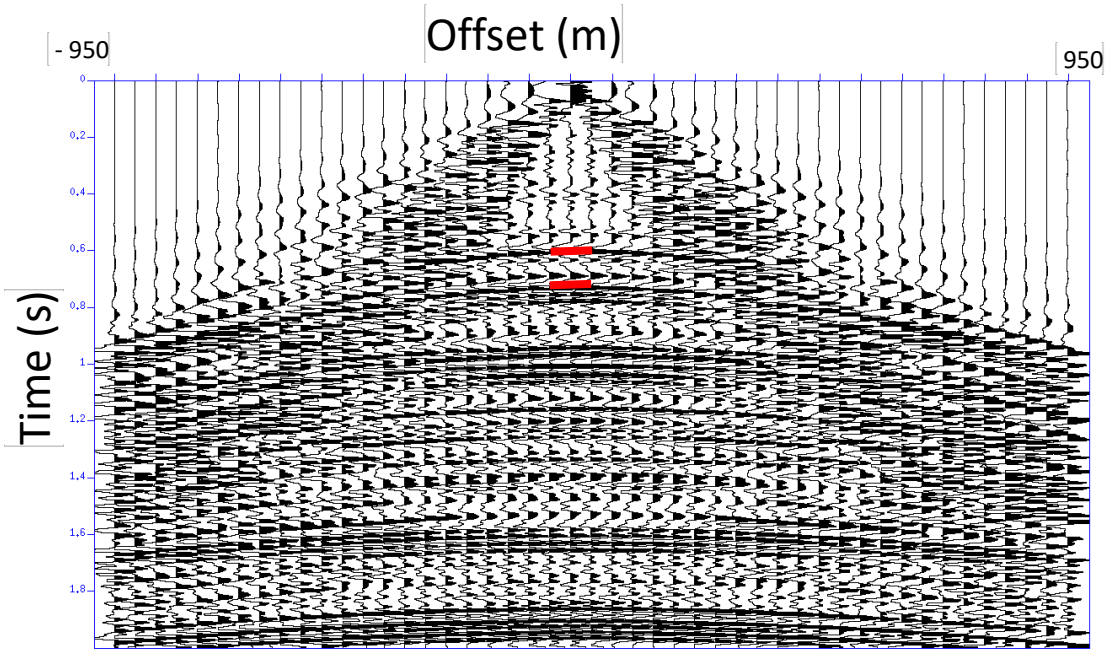

Figure 3.10: The first 2 seconds showing CDP 180000 when short offset is used (top and bottom of Biyadh are shown in red)

Figure 3.11 shows the velocity spectrum of CDP 180000 (all offset):

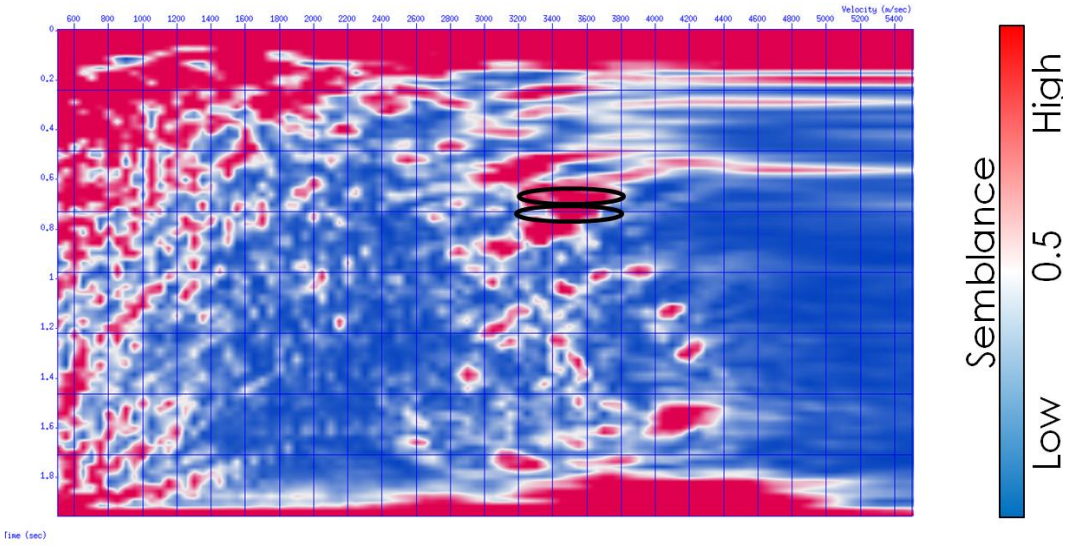

Figure 3.11: Velocity spectrum of CDP 180000 (entire offset). Circles indicate areas of picked velocities.

Figure 3.12 shows the velocity spectrum of CDP 180000 (short offset):

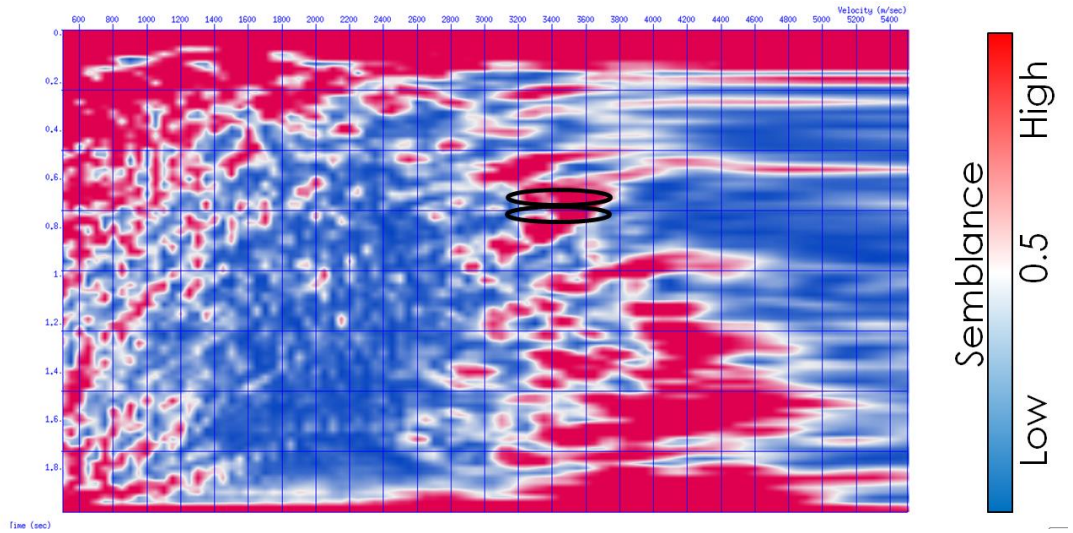

Figure 3.12: Velocity spectrum of CDP 180000 (short offset). Circles indicate areas of picked velocities.

Note that the more reddish areas are in the velocity spectrum means higher semblance. So I started picking my velocities at the areas of high semblance around the times 0.67 s and 0.77 s (around the areas highlighted in circles Figures 3.11 and 3.12) which are the two-way travel times to layers Shuaiba and Biyadh (as I calculated in Table 2.3). This was done so that I can get the velocities of those two layers to use them in Dix formula to calculate the interval velocity of Biyadh. The picking process was done 20 times to make sure that the results are statistically significant. Detailed results of the picks will be shown in the next chapter.

CHAPTER 4

RESULTS

Tables 4.1 and 4.2 show the stacking velocity and time values taken from the 20 picking attempts of my velocity analyses for both long and short offset cases.

Pick Number	Layer	Entire offset T (s)	Entire offset V (m/s)
1	Shuaiba	0.716196	3518.63
1	Biyadh	0.772660	3552.5
2	Shuaiba	0.665676	3395.85
2	Biyadh	0.769688	3514.39
3	Shuaiba	0.674591	3290.01
3	Biyadh	0.775631	3459.36
4	Shuaiba	0.671620	3226.5
4	Biyadh	0.775631	3408.55
5	Shuaiba	0.671620	3256.14
5	Biyadh	0.775631	3472.06
6	Shuaiba	0.671620	3429.72
6	Biyadh	0.775631	3510.16
7	Shuaiba	0.671620	3467.82
7	Biyadh	0.775631	3548.26
8	Shuaiba	0.674591	3493.23
8	Biyadh	0.775631	3577.9
9	Shuaiba	0.674591	3531.33
9	Biyadh	0.775631	3594.83
10	Shuaiba	0.674591	3400.08
10	Biyadh	0.778603	3531.33
11	Shuaiba	0.677563	3480.52
11	Biyadh	0.778603	3484.76
12	Shuaiba	0.677563	3505.93
12	Biyadh	0.778603	3556.73
13	Shuaiba	0.677563	3505.93
13	Biyadh	0.778603	3573.67
14	Shuaiba	0.683507	3556.73
14	Biyadh	0.784547	3518.63
15	Shuaiba	0.671620	3476.29
15	Biyadh	0.772660	3294.24
16	Shuaiba	0.677563	3463.59
16	Biyadh	0.778603	3522.86
17	Shuaiba	0.674591	3446.66
17	Biyadh	0.775631	3323.88
18	Shuaiba	0.667727	3442.39
18	Biyadh	0.769475	3504.12
19	Shuaiba	0.668648	3442.42
19	Biyadh	0.775631	3560.97
20	Shuaiba	0.671620	3404.32
20	Biyadh	0.778603	3514.39

Table 4.1: Picked stacking velocity and time values for long offset

Pick Number	Layer	Short offset T (s)	Short offset V (m/s)
1	Shuaiba	0.662704	3209.57
1	Biyadh	0.769688	3298.48
2	Shuaiba	0.662704	3234.97
2	Biyadh	0.775631	3306.94
3	Shuaiba	0.662704	3387.38
3	Biyadh	0.775631	3505.93
4	Shuaiba	0.665676	3412.79
4	Biyadh	0.775631	3539.8
5	Shuaiba	0.665676	3433.95
5	Biyadh	0.775631	3577.9
6	Shuaiba	0.67162	3467.82
6	Biyadh	0.775631	3590.6
7	Shuaiba	0.674591	3463.59
7	Biyadh	0.778603	3493.23
8	Shuaiba	0.674591	3497.46
8	Biyadh	0.778603	3552.5
9	Shuaiba	0.674591	3510.16
9	Biyadh	0.778603	3556.73
10	Shuaiba	0.677563	3505.93
10	Biyadh	0.778603	3573.67
11	Shuaiba	0.677563	3518.63
11	Biyadh	0.778603	3603.3
12	Shuaiba	0.677563	3544.03
12	Biyadh	0.778603	3628.7
13	Shuaiba	0.668648	3429.72
13	Biyadh	0.77266	3459.36
14	Shuaiba	0.674591	3501.69
14	Biyadh	0.775631	3552.5
15	Shuaiba	0.680535	3522.86
15	Biyadh	0.781575	3573.67
16	Shuaiba	0.674591	3463.59
16	Biyadh	0.778603	3505.93
17	Shuaiba	0.674591	3505.93
17	Biyadh	0.77266	3535.56
18	Shuaiba	0.677563	3510.16
18	Biyadh	0.778603	3582.13
19	Shuaiba	0.73997	3480.52
19	Biyadh	0.77266	3510.16
20	Shuaiba	0.664547	3399.29
20	Biyadh	0.775835	3541.71

Table 4.2: Picked stacking velocity and time values for short offset

Figure 4.1 shows a plot of the picked stacking velocities distribution for entire offset.

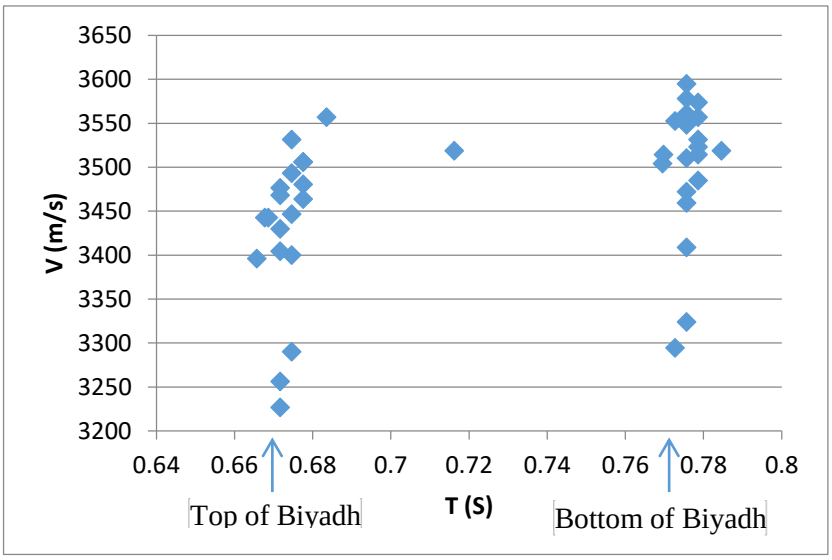

Figure 4.1: Picked stacking velocities for entire offset

Figure 4.2 shows a plot of the picked stacking velocities distribution for short offset.

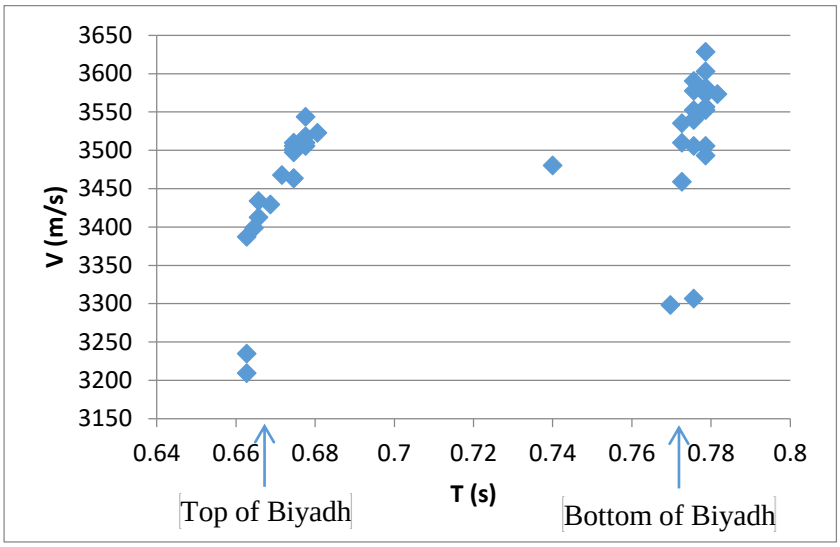

Figure 4.2: Picked stacking velocities for short offset

Note that if I calculate V_{RMS} using equation (1.6) directly in terms of the properties of subsurface layers given in the model, it will be 2932 m/s to the top of Biyadh and 3095 m/s to the bottom of Biyadh. However, it is clear from Figures 4.1 and 4.2 that the values of picked stacking velocities (which should be almost equal to V_{RMS}) are much higher than the model values. Which could be a probable source of error in further calculations.

Utilizing the velocity and time values from Tables 4.1 and 4.2, I used Dix Formula (equation 1.8) to calculate the values of interval velocity corresponding to each stacking velocity and time pick at the top and bottom of Biyadh. Then, I calculated their errors relative to the true interval velocities taken from the model. The results are shown in Table 4.3.

AverageVp (m/s) of Biaydh Taken from the Model (Table 2.1)	Calculated Vi (Dix) For Entire Offset	Vi Error % For Entire Offset	Calculated Vi (Dix) For Short Offset	Vi Error % For Short Offset
4045	3957	2.175	3803	8.5
4045	4194	3.695	3701	2.192
4045	4427	9.444	4134	4.525
4045	4407	8.939	4228	7.511
4045	4630	14.46	4349	6.3
4045	3991	1.342	4300	9.032
4045	4029	0.391	3680	3.817
4045	4099	1.326	3891	4.942
4045	3993	1.286	3845	1.152
4045	4286	5.96	3998	2.013
4045	3513	13.151	4126	2.648
4045	3880	4.073	4152	9.91
4045	3998	1.152	3644	4.21
4045	3804	5.947	3875	3.617
4045	4503	11.324	3899	6.823
4045	3897	3.656	3769	7.713
4045	4175	3.211	3733	0.329
4045	3885	3.956	4032	1.965
4045	4227	4.506	4124	6.18
4045	4139	2.325	4295	5.978
Average	4101.7	5.116	3978.9	4.968
Median	4064	3.826	3948.5	4.734
Standard Deviation	265.407	4.190	224.660	2.772
Max	4630	14.46	4349	9.91
Min	3513	0.391	3644	0.329

Table 4.3: Interval velocities and their errors for long and short offsets

The error was calculated using the following formula:

$$\text{Error} = \left| \frac{\text{Calculated Vi (Dix)} - \text{AverageVp of Biaydh Taken from the model}}{\text{AverageVp of Biaydh Taken from the model}} \right| \text{X } 100$$

Figure 4.3 shows a plot of the calculated interval velocities using Dix Formula.

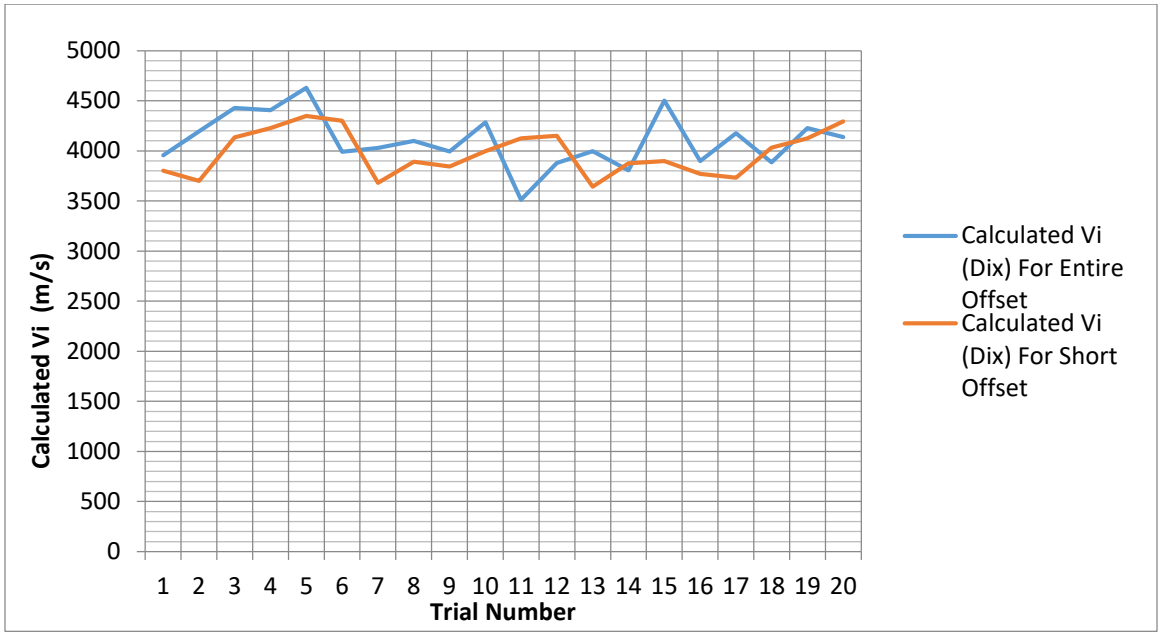

Figure 4.3: Calculated interval velocities

Figure 4.4 shows a plot of the errors percentages for each calculated velocity.

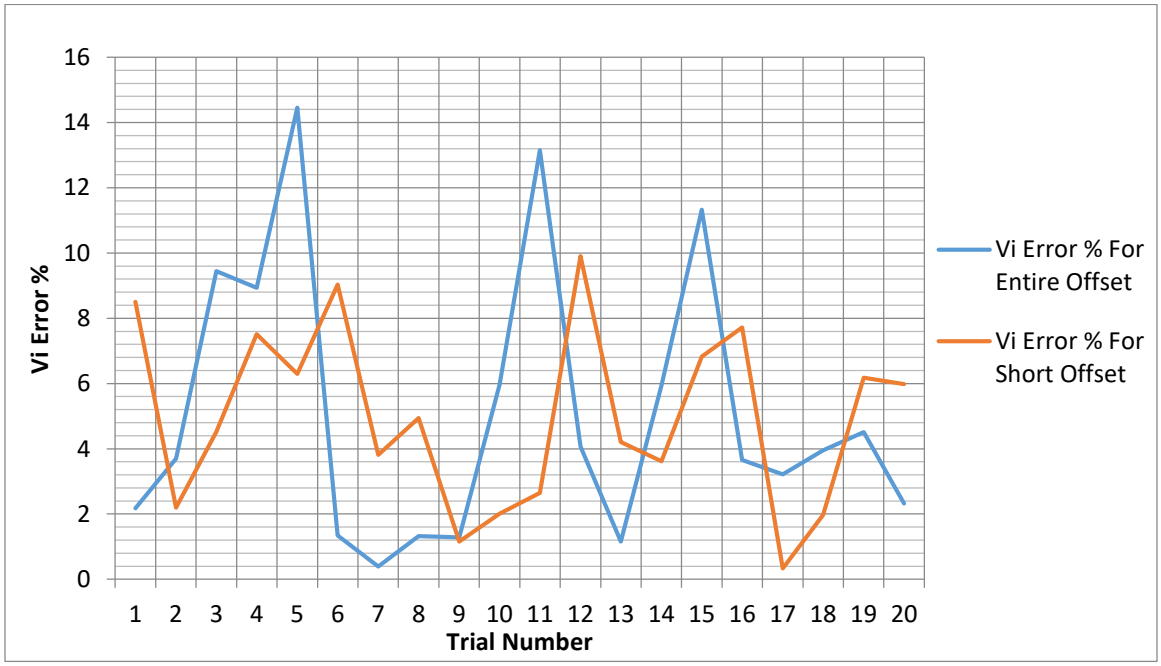

Figure 4.4: Errors in calculated interval velocities

Figure 4.3 shows that most interval velocities values calculated using Dix Formula are clustered around 4000 m/s – which is close enough to the model value of 4045 m/s – for both long and short offset cases. Though there are more outliers in the long offset case.

From this I can infer that the calculated values are almost correct, which in turn means that the methodology used, and the processing done are good enough.

This is further illustrated by looking at Figure 4.4 which shows the errors percentages for each calculated velocity for both long and short offset cases, which are quite low in general. Though there are more outliers in the long offset case too.

CHAPTER 5

DISCUSSION AND CONCLUSIONS

It can be seen from Table 4.3 that there is not much difference between the average velocity error values of the long and the short-offset cases. For the long-offset the average error was 5.116%, and for the short-offset the error was 4.968%. The difference in percentage between the two errors is just 2.893%.

The difference between median values of velocity errors for both cases is also relatively small. It is 3.826% for long-offset, and 4.734% for short-offset. The difference in percentage between those two values is 23.73%.

From my results I can conclude that - unlike what is expected by theory - there is no need to honor the short-offset assumption when working on this area of Ghawar Field.

A possible reason for this result is that the velocity changes gradually from the surface to Biyadh resulting in a true ray path that approximates a straight ray path regardless of the offset.

However, I can see from Figures 3.11 and 3.12 that when looking at layers which are deeper than Biyadh, honoring the short-offset assumption could still make it easier to pick the correct velocities using velocity spectrum method, as it shows better semblance. That is because of better hyperbolic fitting with less noise.

Keep in mind that there is a considerable difference between the standard deviation values of both cases (4.190% and 2.772%) which shows that my data is widely spread. Note that the maximum error for the long offset case is higher than the one for short offset (14.46% and 9.91%). However, the minimum errors for both cases are almost the same (0.391% and 0.329%).

These are some probable sources of errors in the calculations:

1- When processing the data, I tried to simulate an industrial processor using a conventional processing workflow. However, the synthetic data I used was viscoelastic dataset to simulate real data. Therefore, my conventional processing workflow might not be optimum for this complex dataset.
2- Though I was working on a viscoelastic dataset, I was looking only at P waves. There could be some interference from shear waves close to my analysis area.
3- Absorption could change frequency with time, which might have effects that were not accounted for in processing.
4- Noise was added to the synthetic data to simulate real data, which might have affected the results.

For future studies, I recommend the following:

1- Regenerating the data set as acoustic not viscoelastic.
2- Using 3D synthetics.
3- Using other velocity analysis methods such as constant-velocity stacks (CVS).
4- Testing the proposed analysis on real data with well-log information.
5- Calculating the errors in velocity estimation of other layers, and in other areas of Ghawar Field.
6- Using Advanced prestack noise removal methods might give better results.

REFERENCES

Al-Chalabi, M. (1974). An analysis of stacking, RMS, average, and interval velocities over a horizontally layered ground. Geophysical prospecting, 22(3), 458-475.

Al-Chalabi, M. (1973). Series approximation in velocity and traveltime computations. Geophysical prospecting, 21(4), 783-795.

Al-Shuhail, A. A. (2017), Time-Distance (T-X) Curves of Primary Reflections, lecture notes, Seismic Exploration I GEOP315 King Fahd University of Petroleum and Minerals. Available from: http://faculty.kfupm.edu.sa/ES/ashuhail/.

Al-Shuhail, A. A., Alshuhail, A. A., and Khulief, Y. A. (2014). CO2 Leakage Detection using Geophysical Methods under Arid Near-surface Conditions: Progress Report of KACST TIC-CCS Project number TIC-CCS-1, 47 pp.

Causse, E., Haugen, G. U., & Rommel, B. E. (2000). Large-offset approximation to seismic reflection traveltimes. Geophysical prospecting,48(4), 763-778.

Dix, C. H. (1955). Seismic velocities from surface measurements. Geophysics, 20(1), 68-86.

Hake, H., Helbig, K., & Mesdag, C. S. (1984). Three-term Taylor series for t 2-x 2-curves of P-and S-waves ober layered transversely isotropic ground. Geophysical Prospecting, 32(5), 828-850.

Shah, P. M., & Levin, F. K. (1973). Gross properties of time-distance curves. Geophysics, 38(4), 643-656.

Sheriff, R. E., & Geldart, L. P. (1995). Exploration Seismology. New York, NY: Cambridge University Press.

Taner, M. T., & Koehler, F. (1969). Velocity spectra-digital computer derivation applications of velocity functions. Geophysics, 34(6), 859-881.

Thorbecke, J. (2017). fdelmodc: 2D Finite-Difference Wavefield Modelling. TUDelft. Available from: https://janth.home.xs4all.nl/.

Vitae

Name	: Khalid Ahmed Abdulrahman
Nationality	: Saudi
Date of Birth	:11/25/1985
Email	: khalidaaq@hotmail.com khalidaaq@kfupm.edu.sa
Address	: House 5178, Qatif Street, Dhahran, Saudi Arabia.
Academic Background	: B.S. in Computer Science, 2008, King Fahd University of Petroleum and Minerals, Dhahran, Saudi Arabia.